Conditional statistics of temperature fluctuations in turbulent convection

Emily S. C. Ching and K. L. Chau
Department of Physics, The Chinese University of Hong Kong, Shatin, Hong Kong
(Received 28 August 2000; published 28 March 2001)

We find that the conditional statistics of temperature difference at fixed values of the locally averaged temperature dissipation rate in turbulent convection become Gaussian in the regime where the mixing dynamics is expected to be driven by buoyancy. Hence, intermittency of the temperature fluctuations in this buoyancy-driven regime can be solely attributed to the variation of the locally averaged temperature dissipation rate. We further obtain the functional behavior of these conditional temperature structure functions. This functional form demonstrates explicitly the failure of dimensional agruments and enhances the understanding of the temperature structure functions.

DOI: 10.1103/PhysRevE.63.047303 PACS number(s): 47.27.−i, 05.40.−a

In turbulent fluid flows, physical quantities such as velocity, temperature, and pressure exhibit seemingly irregular fluctuations both in time and in space. A key issue in turbulence research is to make sense of these fluctuations. The central result of the seminal work of Kolmogorov in 1941 (K41) [1] is that the fluctuating velocity field in high Reynolds number Navier-Stokes turbulence is self-similar at scales within the inertial range, the range of length scales that are smaller than those of energy input and larger than those affected directly by molecular dissipation. K41 predicted that the velocity structure functions $\langle [u(x+r)-u(x)]^p \rangle$ scale as r^{ξ_p} with scaling exponents ξ_p equal to $p/3$ when r is within the inertial range. Experimental and numerical results, however, indicate that ξ_p is a nonlinear function of p and that turbulent velocity fluctuations are scale dependent in that the shape of the probability density function (PDF) of the velocity difference $u(x+r)-u(x)$ changes with the scale r even when r is within the inertial range. This deviation from the K41 results is associated with intermittency or the uneven distribution of turbulent activity of the velocity field in time and in space.

Extensive efforts have been devoted to understanding the problem of intermittency or anomalous scaling. In his refined similarity hypothesis (RSH) [2,3], Kolmogorov attributed this intermittent nature of the velocity fluctuations to the spatial variations of the energy dissipation rate. Various models have been put forth for the statistics of the locally averaged energy dissipation rate. The most recent model of She and Leveque [4] proposed a hierarchical structure for the moments, which leads to predictions that are in good agreement with experiments. This moment hierarchy was later shown to be naturally satisfied by log-Poisson statistics [5,6].

High Rayleigh number convection has been a well-studied model system for investigating turbulence. Fluid motion is driven by an applied temperature difference across the top and bottom plates of a closed experimental cell filled with fluid. The temperature field in convection is thus a so-called active scalar. The flow state is characterized by the geometry of the cell and two dimensionless parameters: the Rayleigh number $\mathrm{Ra}=\alpha g \Delta L^3/(\nu\kappa)$ and the Prandtl number $\mathrm{Pr}=\nu/\kappa$, where L is the height of the cell, Δ the applied temperature difference, g the acceleration due to gravity, and α, ν, and κ are, respectively, the volume expansion coefficient, the kinematic viscosity, and the thermal diffusivity of the fluid. When Ra is large enough, the convection becomes turbulent.

In turbulent convection, the temperature fluctuations are also intermittent [7]. As for velocity fluctuations in high Reynolds number Navier-Stokes turbulence, it is of interest to understand the intermittency of temperature fluctuations in high Rayleigh number convection. Turbulent convection poses additional interesting questions of its own. There is the issue of whether and how the characteristics of turbulence are affected by the presence of buoyancy. One expects the mixing dynamics to be driven by buoyancy at scales larger than the Bolgiano scale, $l_B \equiv \overline{\epsilon}^{5/4}/[\overline{\chi}^{3/4}(\alpha g)^{3/2}]$ [8], where $\overline{\epsilon}$ and $\overline{\chi}$ are, respectively, the average energy and temperature (variance) dissipation rates. On the other hand, for length scales smaller than l_B, the mixing dynamics is expected to be driven by the inertial force of the fluid motion and the temperature field is effectively passive. Recently, one of us (Ching) [9] has analyzed the intermittency of the temperature field in turbulent convection. The normalized temperature structure functions have indeed been found to have different scaling exponents in the buoyancy-driven and inertia-driven regimes.

In our present project, we attempt to understand the intermittency problem of temperature by separating it into two parts: the understanding of the conditional statistics of temperature fluctuations at fixed values of the locally averaged temperature dissipation rate and the understanding of the statistics of the local temperature dissipation. In this Brief Report, we report our study of the first part. The second part of our study is reported elsewhere [10]. This separation allows us to address especially whether the RSH type of ideas would be fruitful. We shall see that the intermittent nature of the temperature fluctuations in the buoyancy-driven regime can indeed be attributed to variations of the locally averaged temperature dissipation rate. Moreover, a change in the statistical features of the temperature fluctuations is again observed when the Bolgiano scale l_B is crossed. This change manifests itself as a change in the behavior of the conditional PDFs of the temperature difference at a fixed value of the locally averaged temperature dissipation rate.

We use temperature data obtained by Libchaber and coworkers in the well-documented experiment on low-temperature helium gas [11,12] for our analyses. The experimental cell heated from below is cylindrical with a diameter of 20 cm and a height of 40 cm. A mean circulating flow is present for $\mathrm{Ra} \geq 10^8$. The temperature at the center of the cell, $T(t)$, was measured as a function of time t. We evaluate the temperature difference between two times: $T_\tau(t) \equiv T(t+\tau) - T(t)$. The intermittency of the temperature fluctuations is manifested as a change in the shape of the PDF of T_τ as τ varies. In our earlier study of this τ dependence [7], the dissipative and the circulation time scales, τ_d and τ_c, were identified. A time scale corresponding to l_B is naturally defined by $\tau_B = \tau_c\, l_B / L$. It was shown [13] that l_B can be written as

$$l_B = \frac{\mathrm{Nu}^{1/2} L}{(\mathrm{Ra}\,\mathrm{Pr})^{1/4}} \tag{1}$$

where the Nusselt number (Nu) is the heat flux normalized by that when there is only conduction. Thus, τ_B can easily be evaluated using the measured values of Nu, Ra, and Pr.

The locally averaged temperature dissipation rate χ_r is the spatial average of $\kappa |\nabla T|^2$ over a ball of radius r. We estimate it by χ_τ, which is defined as

$$\chi_\tau(t) \equiv \frac{1}{\tau} \int_t^{t+\tau} \frac{\kappa}{\langle u_c^2 \rangle} \left(\frac{\partial T}{\partial t'} \right)^2 dt' \tag{2}$$

and can be calculated using one-point temperature measurements. Here, $\langle u_c^2 \rangle$ is the mean square velocity fluctuation at the center of the cell.

We start by investigating the conditional PDF of T_τ, at fixed values of χ_τ. We consider those $T_\tau(t)$ whose corresponding $\ln \chi_\tau(t)$ assumes a certain value within a small range δ, and calculate the conditional PDFs $P(Y_\tau | \chi_\tau)$ where

$$Y_\tau \equiv \frac{T_\tau}{\sqrt{\langle T_\tau^2 | \chi_\tau \rangle}}. \tag{3}$$

As the conditional mean $\langle T_\tau | \chi_\tau \rangle$ is approximately zero, $P(Y_\tau|\chi_\tau)$ is standardized with zero mean and unit standard deviation. For a given τ, $P(Y_\tau|\chi_\tau)$ is found to be independent of χ_τ for a range of χ_τ that contains most of the data. The conditional PDFs for different values of τ are plotted in Fig. 1. We measure the value of χ_τ in units of $\chi \equiv \kappa \langle (\partial T/\partial t)^2 \rangle / \langle u_c^2 \rangle$. In the limit $\tau \rightarrow 0$, $\chi_\tau \sim T_\tau^2$; therefore the conditional PDF is bimodal for small τ, as seen in the figure. As τ increases, $P(Y_\tau|\chi_\tau)$ changes from bimodal to a function with one maximum and varies with τ, but for larger τ it becomes a standardized Gaussian distribution and is thus independent of τ. Such a change in behavior occurs at $\tau \approx \tau_B$.

Hence, a change in the statistical features of the temperature fluctuations is again observed as the Bolgiano scale is crossed, demonstrating that buoyancy does have an effect on the characteristics of turbulence in convection. Moreover, the physical nature of the presently observed change is clear. We have the interesting result that the temperature fluctuations at fixed values of χ_τ become self-similar and thus nonintermittent in the regime where the mixing dynamics is expected to be driven by buoyancy. In other words, intermittency of the temperature fluctuations in this buoyancy-driven regime can be solely attributed to the variations of χ_τ.

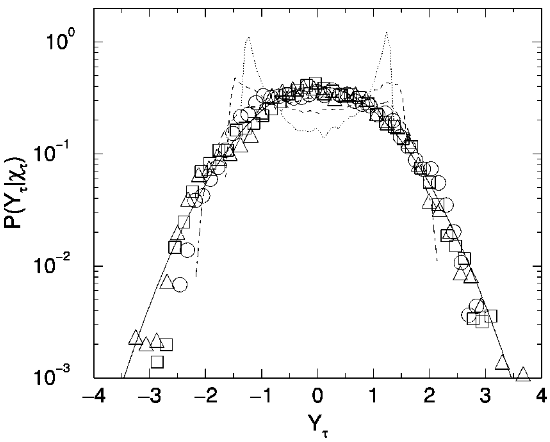

FIG. 1. The conditional PDFs $P(Y_\tau|\chi_\tau)$ versus Y_τ for $\mathrm{Ra}=6.0\times10^{11}$ and $\chi_\tau/\chi=0.18$ for various values of τ. $\tau=8$ (dotted line), $\tau=16$ (dashed line), $\tau=32$ (dot-dashed line), $\tau=64$ (circles), $\tau=128$ (squares), and $\tau=256$ (triangles). It can be seen that $P(Y_\tau|\chi_\tau)$ becomes a standard Gaussian distribution (solid line) for $\tau>\tau_B\approx70$. All times are in units of the sampling time $=1/409.6$ s. The conditional PDFs are found to be independent of χ_τ.

In the remainder of this Brief Report, we shall obtain the functional dependence of the conditional temperature structure functions $\langle |T_\tau|^p | \chi_\tau \rangle$ on p, τ, and χ_τ.

It is illuminating to first work out what functional form is predicted by simple phenomenology and dimensional agruments. One expects T_r, the temperature difference across a scale r, to depend on r, χ_r, and u_r, the velocity difference across the same scale r. In the inertia-driven regime, u_r is related to the locally averaged energy dissipation rate ϵ_r by $u_r \sim (r\epsilon_r)^{1/3}$, while in the buoyancy-driven regime, u_r is generated by buoyancy: $u_r^2/r \sim \alpha g T_r$. Hence, we have

$$T_r \sim \begin{cases} r^{1/3} \epsilon_r^{-1/6} \chi_r^{1/2}, & r < l_B \\ r^{1/5} \chi_r^{2/5} (\alpha g)^{-1/5}, & r > l_B. \end{cases} \tag{4}$$

Equation (4) implies that

$$\langle |T_\tau|^p | \chi_\tau \rangle \sim \begin{cases} \langle u_c^2 \rangle^{p/6} \tau^{p/3} \chi_\tau^{p/2} \langle \epsilon_\tau{}^{-p/6} | \chi_\tau \rangle, & \tau < \tau_B \\ \langle u_c^2 \rangle^{p/10} \tau^{p/5} \chi_\tau^{2p/5} (\alpha g)^{-p/5}, & \tau > \tau_B, \end{cases} \tag{5}$$

if T_τ, χ_τ, and ϵ_τ have the same scaling behavior in τ as the corresponding quantities with subscript r in r with $r = \langle u_c^2 \rangle^{1/2} \tau$.

If the variations of χ_τ and ϵ_τ are both ignored, Eq. (5) implies that the temperature frequency power spectrum has a scaling $\omega^{-7/5}$ for frequency $\omega < \omega_B$ and $\omega^{-5/3}$ for $\omega > \omega_B$, where $\omega_B = 2\pi/\tau_B$. The former scaling behavior was reported for the temperature frequency power spectra measured in water [13] and helium [14] while the latter was reported for that measured in low Pr mercury [15].

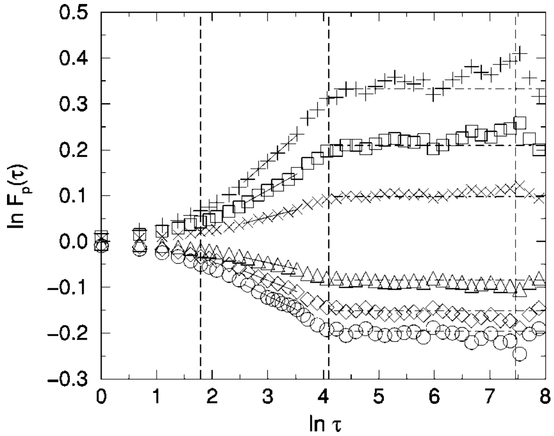

FIG. 2. The logarithm of the normalized conditional temperature structure functions $F_p(\tau) \equiv \langle |T_\tau|^p | \chi_\tau \rangle / \langle T_\tau^2 | \chi_\tau \rangle^{p/2}$ versus $\ln \tau$ for $\mathrm{Ra} = 7.3 \times 10^{10}$ and $\chi_\tau/\chi = 0.43$ for various values of p. The three time scales τ_d, τ_B, and τ_c are approximately 6, 60, and 1750, respectively, and are indicated by the dashed lines. All times are in units of the sampling time $= 1/320$ s. $p = 0.5$ (circles), $p = 1.5$ (diamonds), $p = 1.75$ (triangles), $p = 2.25$ (crosses), $p = 2.5$ (squares), and $p = 2.75$ (pluses). For $\tau_d < \tau < \tau_B$, $F_p(\tau)$ can be fitted by a power law $C_p \tau^{\alpha_p}$ (solid lines) and for $\tau > \tau_B$ it becomes $\sqrt{2^p/\pi}\,\Gamma[(p+1)/2]$ (dot-dashed lines) and is thus independent of τ.

Now we proceed with the analyses. From the result that $P(Y_\tau | \chi_\tau)$ is independent of χ_τ, we get

$$\langle |T_\tau|^p | \chi_\tau \rangle = F_p(\tau) \sigma^p(\tau, \chi_\tau), \tag{6}$$

where

$$\sigma(\tau, \chi_\tau) \equiv \sqrt{\langle T_\tau^2 | \chi_\tau \rangle}. \tag{7}$$

By definition, $F_2(\tau) = 1$. For $\tau > \tau_B$, $P(Y_\tau | \chi_\tau)$ becomes a standardized Gaussian; thus

$$F_p(\tau > \tau_B) = \sqrt{\frac{2^p}{\pi}} \Gamma\left(\frac{p+1}{2}\right) \tag{8}$$

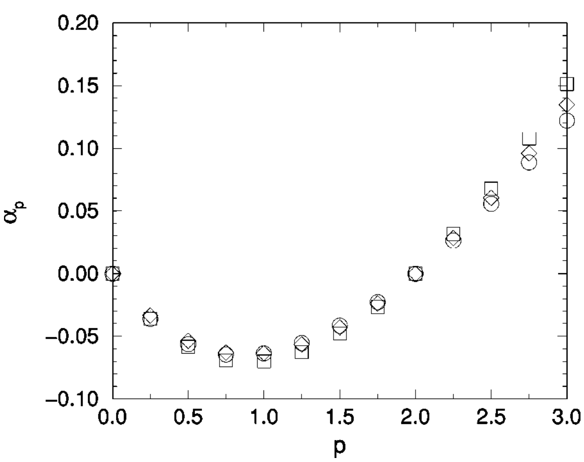

FIG. 3. The scaling exponent α_p versus p for $\mathrm{Ra} = 4.0 \times 10^9$ (circles), $\mathrm{Ra} = 7.3 \times 10^{10}$ (squares), and $\mathrm{Ra} = 6.0 \times 10^{11}$ (diamonds).

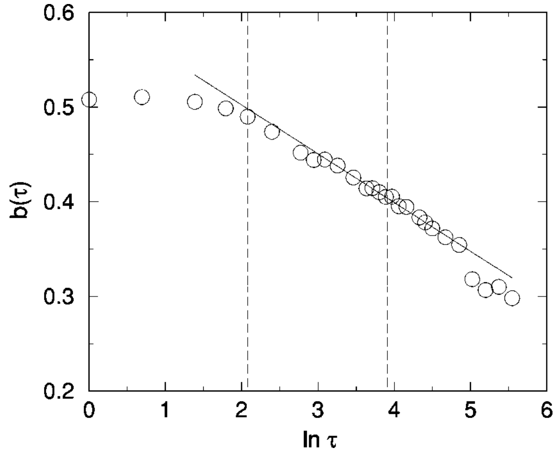

FIG. 4. The scaling exponent $b(\tau)$ versus $\ln \tau$ for $\mathrm{Ra} = 4.0 \times 10^9$. The time scales τ_d and τ_B are approximately 8 and 50, respectively, and are indicated by the dashed lines. All times are in units of the sampling time $= 1/160.8$ s. It can be seen that $b(\tau)$ is close to 1/2 for $\tau \leq \tau_d$ and can be fitted by a linear function in $\ln \tau$ (solid line) for $\tau > \tau_d$. Moreover, $b(\tau) \approx 2/5$ at $\tau \approx \tau_B$.

is independent of τ. For $\tau_d < \tau < \tau_B$, we find that $F_p(\tau)$ can be fitted by a power law (see Fig. 2), that is,

$$F_p(\tau) \approx C_p \tau^{\alpha_p}, \quad \tau_d < \tau < \tau_B. \tag{9}$$

This τ dependence of F_p echoes that of $P(Y_\tau | \chi_\tau)$ for $\tau < \tau_B$. Using Eq. (5), such dependence can be attributed to the additional variation of the local energy dissipation rate ϵ_τ even when the local temperature dissipation rate χ_τ is held fixed. The scaling exponents α_p are plotted in Fig. 3. Since $\alpha_0 = \alpha_2 = 0$ by definition, α_p has to be a nonlinear function of p, as is found.

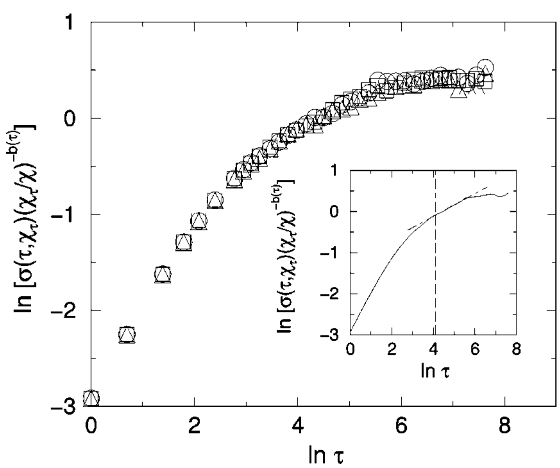

FIG. 5. $\ln \sigma(\tau, \chi_\tau)(\chi_\tau/\chi)^{-b(\tau)}$ versus $\ln \tau$ for $\mathrm{Ra} = 7.3 \times 10^{10}$ for $\chi_\tau/\chi = 0.13$ (circles), $\chi_\tau/\chi = 0.35$ (squares), and $\chi_\tau/\chi \approx 0.96$ (triangles). The three sets of data collapse into a single function of $\tau [= G(\tau) \chi^{b(\tau)}]$ confirming Eq. (10). The times are in units of the sampling time $= 1/320$ s while σ is in units of the standard deviation of the temperature fluctuations. Shown in the inset is the average of the three sets of data (solid line), which can be fitted by a power law (dot-dashed line) for $\tau > \tau_B$ (indicated by dashed line).

Next, we analyze the functional dependence of σ. We fix τ and study its dependence on χ_τ. When τ is not too large, $\sigma(\tau,\chi_\tau)$ indeed scales with χ_τ for a range of χ_τ that contains most of the data. The scaling exponent $b(\tau)$, however, varies with τ. When τ is large, the data scatter. Thus, we have

$$\sigma(\tau,\chi_\tau)=G(\tau)\chi_\tau^{b(\tau)}. \tag{10}$$

From the relation $\chi_\tau \sim T_\tau^2$ in the limit of $\tau\to 0$, one gets $b(\tau)\to 1/2$ as $\tau\to 0$. Indeed, as shown in Fig. 4, $b(\tau)$ is about 1/2 for $\tau \leq \tau_d$. It then crosses over to an approximately linear function of $\ln\tau$, and has a value of 2/5 at $\tau\approx\tau_B$. This is, therefore, in contrast to the behavior of $\sigma(\tau,\chi_\tau)\sim\tau^{1/3}\chi_\tau^{1/2}$ and $\sigma(\tau,\chi_\tau)\sim\tau^{1/5}\chi_\tau^{2/5}$, respectively, in the inertia-driven ($\tau_d<\tau<\tau_B$) and buoyancy-driven regimes ($\tau_B<\tau<\tau_c$) that simple phenomenology and dimensional agruments would predict [see Eq. (5)]. In Fig. 5, we plot $\sigma(\tau,\chi_\tau)(\chi_\tau/\chi)^{-b(\tau)}$ for various values of χ_τ. The linear fit of $b(\tau)$ in $\ln\tau$ is used for $\tau>\tau_d$. The data for different values of χ_τ collapse to one single curve, thus confirming Eq. (10). We take the average of the data to get an estimate of $G(\tau)\chi^{b(\tau)}$, which is shown in the inset. It can be fitted by a power law for $\tau>\tau_B$ with an exponent about 0.27.

The temperature structure functions $\langle|T_\tau|^p\rangle$ are related to the conditional ones at fixed values of χ_τ as follows:

$$\langle|T_\tau|^p\rangle=\int_0^\infty\langle|T_\tau|^p|\chi_\tau\rangle P_\tau(\chi_\tau)d\chi_\tau, \tag{11}$$

where $P_\tau(\chi_\tau)$ is the PDF of χ_τ. Using Eqs. (6) and (10), we thus get

$$\langle|T_\tau|^p\rangle=F_p(\tau)G^p(\tau)\langle\chi_\tau^{pb(\tau)}\rangle. \tag{12}$$

Equation (12) implies that the change in the scaling exponent of the normalized structure functions $\langle|T_\tau|^p\rangle/\langle T_\tau^2\rangle^{p/2}$ observed when τ_B is crossed [9] is the combined effect of the changes in the τ dependence of $F_p(\tau)$ and $\langle\chi_\tau^{pb(\tau)}\rangle$. The comparison of Eq. (12) with data will be presented elsewhere.

In summary, we have studied systematically the conditional statistics of the temperature fluctuations at fixed values of local temperature dissipation χ_τ in turbulent convection. We have found that such conditional statistics become self-similar in the buoyancy-driven regime, demonstrating that the intermittency of the temperature field in this regime can be attributed solely to the variations of χ_τ. We have worked out the functional behavior of the conditional structure functions $\langle|T_\tau|^p|\chi_\tau\rangle$. There is indeed scaling behavior in χ_τ but the scaling exponent $b(\tau)$ depends on τ, contrary to what simple phenomenology and dimensional agruments might predict. We emphasize that this τ dependence demonstrates explicitly the failure of dimensional arguments. Together with the knowledge of the statistical properties of χ_τ, this functional behavior should enable us to better understand the temperature structure functions.

E.S.C.C. would like to acknowledge discussions with T. Witten. This work is supported by a grant from the Research Grants Council of the Hong Kong Special Administrative Region, China (Grant No. CUHK 4119/98P).

[1] A.N. Kolmogorov, C. R. Acad. Sci. URSS **30**, 301 (1941).
[2] A.N. Kolmogorov, J. Fluid Mech. **12**, 82 (1962).
[3] A.M. Obukhov, J. Fluid Mech. **12**, 77 (1962).
[4] Z.-S. She and E. Leveque, Phys. Rev. Lett. **72**, 336 (1994).
[5] B. Dubrulle, Phys. Rev. Lett. **73**, 959 (1994).
[6] Z.-S. She and E.C. Waymire, Phys. Rev. Lett. **74**, 262 (1995).
[7] E.S.C. Ching, Phys. Rev. A **44**, 3622 (1991).
[8] A. S. Monin and A. M. Yaglom, *Statistical Fluid Mechanics* (MIT Press, Cambridge, MA, 1975).
[9] E.S.C. Ching, Phys. Rev. E **61**, R33 (2000).
[10] E. S. C. Ching and C. Y. Kwok, Phys. Rev. E. **62**, R7587 (2000).
[11] F. Heslot, B. Castaing, and A. Libchaber, Phys. Rev. A **36**, 5870 (1987).
[12] M. Sano, X.-Z. Wu, and A. Libchaber, Phys. Rev. A **40**, 6421 (1989).
[13] F. Chiliá, S. Ciliberto, C. Innocenti, and E. Pampaloni, Nuovo Cimento D **15**, 1229 (1993).
[14] X.-Z. Wu, L. Kadanoff, A. Libchaber, and M. Sano, Phys. Rev. Lett. **64**, 2140 (1990).
[15] S. Cioni, S. Ciliberto, and J. Sommeria, Europhys. Lett. **32**, 413 (1995).